Available online at www.sciencedirect.com

ScienceDirect

Journal of the European Ceramic Society 27 (2007) 4103–4106

www.elsevier.com/locate/jeurceramsoc

Growth of (Na, K, Li)(Nb, Ta)O_3 single crystals by solid state crystal growth

John G. Fisher[a], Andreja Benčan[a,*], Janez Bernard[a], Janez Holc[a], Marija Kosec[a], Sophie Vernay[b], Daniel Rytz[b]

[a] *Electronic Ceramics Department, Jožef Stefan Institute, Jamova 39, Ljubljana 1000, Slovenia*
[b] *Forschungsinstitut für mineralische und metallische Werkstoffe Edelsteine/Edelmetalle (FEE) GmbH, Struthstraße 2, D-55743 Idar-Oberstein, Germany*

Abstract

A single crystal of (Na, K, Li)(Nb, Ta)O_3 has been grown for the first time by the solid state crystal growth process. A seed crystal of ⟨0 0 1⟩-oriented $KTaO_3$ was embedded in a matrix of (Na, K, Li)(Nb, Ta)O_3 powder, which was then densified by hot-pressing. During annealing of the hot-pressed sample, a single crystal of (Na, K, Li)(Nb, Ta)O_3 of between 20 and 50 μm thickness grew on the $KTaO_3$ seed. The single crystal contained porosity incorporated from the matrix. Chemical analysis showed the single crystal to have the same composition as the matrix. A single crystal of constant thickness could be grown by adding a liquid phase sintering aid to the powder. The solid state crystal growth method is promising for the growth of single crystals of (Na, K, Li)(Nb, Ta)O_3.

Keywords: Grain growth; Electron microscopy; Microstructure-final; Niobates; Lead-free piezoelectric

1. Introduction

Lead-based ferroelectrics, such as Pb(Zr,Ti)O_3 (PZT) are used in many applications due to their superior piezoelectric properties.[1] However, the volatile and toxic nature of PbO causes problems during processing and environmental problems when the ceramics are disposed of. For these reasons, much work has recently been focused on lead-free ferroelectrics. A promising family of lead-free ferroelectrics is the alkali niobate family. $(K_{0.5}Na_{0.5})NbO_3$ ceramics are suitable candidates for lead-free piezoelectric ceramics.[2,3] However, their properties are inferior to those of PZT ceramics. More recently, ceramics from the (Na, K, Li)(Nb, Ta)O_3 family have been developed.[4] Such ceramics have been found to possess properties similar to those of PZT ceramics.

Work on single crystals from lead-free systems has shown them to possess piezoelectric properties superior to their polycrystalline equivalents when combined with crystallographic engineering techniques.[5] This raises the possibility of producing lead-free piezoelectric single crystals with properties equal or superior to those of PZT. Single crystals of $(Na_{1-x}K_x)NbO_3$ have been grown by the flux method.[6] However, it is difficult to control the composition of single crystals grown by this method. Moreover, single crystal growth for mixed (Na, K, Li)(Nb, Ta)O_3 has yet to be demonstrated for the optimum composition provided in ref. [4].

In a previous paper, the growth of single crystals of $(Na_{0.5}K_{0.5})NbO_3$ by the method of solid state crystal growth was described.[7] In this method, a seed crystal is buried in a powder compact. The sample is then sintered and a single crystal grows using the seed crystal as a template. Because crystal growth takes place in the solid state, this method is suitable for growing crystals of compounds that melt incongruently or which have volatile elements. In the present paper, the growth of single crystals of (Na, K, Li)(Nb, Ta)O_3 by this method will be described.

2. Experimental

Powder of composition $[(Na_{0.5}K_{0.5})_{0.97}Li_{0.03}](Nb_{0.8}Ta_{0.2})O_3$ (composition LF3 in ref. [4]) was prepared by the solid oxide method. Appropriate amounts of K_2CO_3 (Aldrich, >99%),

---

* Corresponding author. Tel.: +386 1 477 3256; fax: +386 1 477 3887.
E-mail address: andreja.bencan@ijs.si (A. Benčan).

0955-2219/$ – see front matter © 2007 Elsevier Ltd. All rights reserved.
doi:10.1016/j.jeurceramsoc.2007.02.101

Na_2CO_3 (Riedel-de Haën, 99.8%), $Li_2C_2O_4$ (Alfa Aesar, >99%), Nb_2O_5 (H.C. Starck, 99.8%) and Ta_2O_5 (H.C. Starck, 99.8%) were attrition milled in acetone with ZrO_2 media. The powder was calcined at 900 °C for 4 h. The calcined powder was examined by powder X-ray diffraction (XRD) and found to be single phase.

$KTaO_3$ single crystals (FEE GmbH, Germany) oriented in the $\langle 0\,0\,1\rangle$ direction were used as seed crystals. A $2\,mm \times 2\,mm \times 0.5\,mm$ seed crystal was buried in 1.2 g of powder. The resulting composite sample was cold pressed at 100 MPa, followed by cold isostatic pressing at 200 MPa. The sample was pre-densified by hot-pressing at 1025 °C and 50 MPa for 2 h. The hot-pressed sample was placed on Pt foil in a closed alumina crucible and annealed in a tube furnace at 1175 °C in air for 10 h. The heating and cooling rates were $5\,°C\,min^{-1}$.

A crystal growth experiment was also carried out with the addition of a liquid phase sintering aid to the powder. $K_4CuNb_8O_{32}$ was used as a liquid phase sintering aid.[8] K_2CO_3, CuO (Alfa Aesar, 99.7%) and Nb_2O_5 were attrition milled as before and calcined at 700 °C for 4 h. XRD of the calcined powder showed it to be single phase. 0.5 mol% of $K_4CuNb_8O_{32}$ was added to the $[(Na_{0.5}K_{0.5})_{0.97}Li_{0.03}](Nb_{0.8}Ta_{0.2})O_3$ powder, followed by attrition milling. A seed crystal was buried in the powder, followed by cold pressing and cold isostatic pressing as before. The sample was hot-pressed at 975 °C and 50 MPa for 2 h, followed by annealing at 1135 °C for 50 h in the tube furnace. The heating and cooling rates were $2\,°C\,min^{-1}$.

Samples were vertically sectioned with a low speed diamond wheel saw and polished to a 0.25 μm finish. Samples were thermally etched, carbon coated and characterized using a scanning electron microscope (SEM, JEOL 5800, Tokyo, Japan) equipped with a LINK ISIS 300 energy-dispersive X-ray spectrometer (EDS). Standard-less quantitative EDS analysis was performed using the SEMQuant program within the Oxford-Link ISIS 300 system, with the virtual standard package (VSP) data library and the ZAF matrix-correction method.

3. Results

SEM micrographs of the sample without the liquid phase sintering aid are shown in Fig. 1. Fig. 1(a) shows the $KTaO_3$ seed crystal, a single crystal layer that has grown on the seed crystal and the matrix. The boundary between the single crystal and the matrix is marked with a dotted black line. The single crystal layer varies in thickness between 20 and 50 μm along the seed crystal. Matrix grains can be seen protruding into the single crystal.

Fig. 1(b) shows the edge of the single crystal and the matrix grains. Square and rectangular pores are visible in the single crystal (marked with arrows). The faces of the pores appear to be parallel with the faces of the single crystal. The matrix grains have a very wide grain size distribution, varying from 1 to over 30 μm in diameter. Both the single crystal and the matrix grains have faceted grain boundaries.

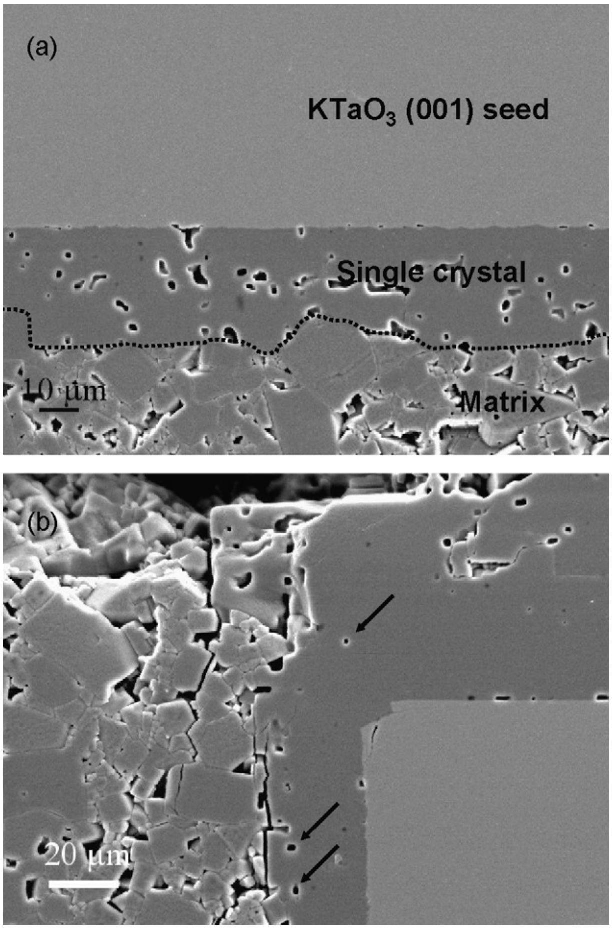

Fig. 1. (a) SEM micrograph of the seed crystal and the grown single crystal layer for the sample without liquid phase sintering aid and (b) SEM micrograph of the edge of the single crystal and the matrix.

For EDS analysis, 6 point measurements of the single crystal and 3 point measurements of the matrix grains were taken. The results are shown in Table 1. The results are presented as the mean value and standard deviation of the cation ratios, normalized to Nb. The composition of the single crystal is identical to that of the matrix grains, within the standard deviations of the measurements. Note that the Na/K ratio is less than 1. When using standard-less analysis the absorption of Na Kα X-rays is not sufficiently corrected for. Also, there is migration of Na away from the electron beam.[9] The Li concentration cannot be measured due to absorption of X-rays characteristic for Li by the detector window.

Table 1
Cation ratios of single crystal and matrix grains measured by SEM–EDS for the sample without liquid phase sintering aid

	Na	K	Nb	Ta
Single crystal	0.505 ± 0.025	0.602 ± 0.020	1 ± 0.000	0.269 ± 0.016
Matrix	0.505 ± 0.040	0.601 ± 0.013	1 ± 0.000	0.281 ± 0.010

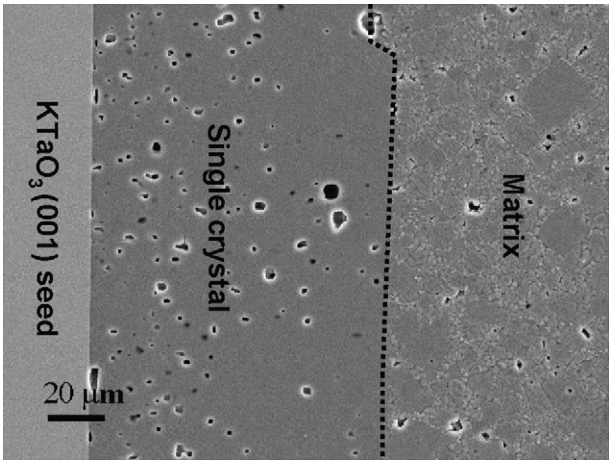

Fig. 2. SEM micrograph of the seed crystal, the grown single crystal layer and the matrix for the sample with liquid phase sintering aid.

A SEM micrograph of the sample with the liquid phase sintering aid is shown in Fig. 2. A single crystal layer ~110 μm thick has grown upon the seed crystal. Crystal growth is uniform across the face of the seed crystal. As before, porosity is present in both the single crystal and the matrix. The matrix has a wide grain size distribution, with abnormal grains up to 20 μm in diameter. EDS analysis indicates that the single crystal and the matrix grains have the same composition. Both the single crystal and the matrix grains have faceted grain boundaries.

4. Discussion

When a ceramic body is sintered, grain growth occurs. Grain growth can be classified as normal or abnormal. In normal grain growth, the mean grain size increases but the shape of the grain size distribution is unchanged. In abnormal grain growth, a few grains grow at a much faster rate than the surrounding matrix grains and a bimodal grain size distribution emerges. Solid state crystal growth is a deliberately induced form of abnormal grain growth, in which the seed crystal effectively acts like a large grain which grows rapidly by consuming the surrounding matrix grains.

Grain growth is dependent on both the driving force for grain growth and the nature of the interfaces (grain boundaries or solid/liquid interfaces). For solid state sintered ceramics, the driving force is the change in the chemical potential of atoms across a curved grain boundary.[10] The driving force for grain growth is proportional to the difference between the radius of the growing grain and the mean size of the grains surrounding it (usually taken to be the mean grain size of the whole matrix).[11] For liquid phase sintered ceramics, the driving force is the difference in solubility between different sized grains in the liquid phase. The driving force is proportional to the difference in size between the growing grain and the mean grain size.[12] The variation of grain growth rate with increasing driving force is governed by the nature of the interfaces.[11,12] If the interfaces are atomically rough, then atoms can easily attach at any point on the interface. The grain growth rate is linearly proportional to the driving force for grain growth. In this case, all grains larger than the mean grain size can grow and a unimodal grain size distribution develops without abnormal grain growth. In such a case, solid state crystal growth will not take place.[13] If the interfaces are atomically smooth or faceted, then atoms can only attach to the interface if a ledge generating source, such as a 2-dimensional (2D) nucleus is present. These 2D nuclei are thermodynamically unstable at low driving forces.[14] The grain growth rate is now an exponential function of the driving force. The grain growth rate is very slow until a critical driving force is reached, at which point the 2D nuclei are thermodynamically stable. The grain growth rate will then increase rapidly to reach the equivalent value for a rough interface. In this case, grains that are large enough to have a driving force greater than the critical driving force can grow rapidly and a bimodal grain size distribution develops with small matrix grains and large abnormal grains.[13] In such a case, solid state crystal growth can take place.

This correlation between interface structure and grain growth behaviour can be clearly seen in Figs. 1 and 2. The interfaces are faceted, and it is seen that solid state crystal growth has taken place on the seed crystal. Due to its large size, the seed crystal had a driving force greater than the critical driving force and could grow rapidly. In addition, abnormal grain growth has taken place in the matrix, with a bimodal distribution of small grains and large abnormal grains. Some of the matrix grains were also large enough to grow rapidly, forming abnormal grains.

The EDS results show that the composition of the single crystal and of the matrix grains is almost identical. This means that the solid state crystal growth method can successfully be used to grow single crystals of complex composition without segregation of the components. Differences in composition from point to point (i.e. the standard deviation in the measurements) may reflect slight inhomogeneities in the starting powder.

The growth rate of the single crystal was rather slow and also not constant across the seed crystal in the sample without a liquid phase sintering aid. Addition of the liquid phase sintering aid resulted in more uniform single crystal growth across the seed. Crystal growth was still rather slow even with the addition of a liquid phase sintering aid. This is probably due to grain growth in the matrix. As the mean matrix grain size increases, the driving force for single crystal growth decreases.[12] To maintain the driving force for single crystal growth, grain growth in the matrix needs to be suppressed. Porosity was present in both the matrix and the single crystal. The sample may not have completely densified during hot-pressing. The faces of the pores are parallel with the faces of the single crystal. The faces of the single crystal should be $\{0\,0\,1\}$ faces due to the $\langle 0\,0\,1\rangle$ orientation of the seed. This, along with the cubic shape of the pores, suggests that in $[(Na_{0.5}K_{0.5})_{0.97}Li_{0.03}](Nb_{0.8}Ta_{0.2})O_3$ the $\{1\,0\,0\}$ faces have a lower surface energy than the other crystal faces, as has also been suggested for single crystalline[7] and polycrystalline $(Na_{0.5}K_{0.5})NbO_3$.[15] Future work will concentrate on reducing grain growth and porosity in the matrix in order to increase the size and density of the single crystals.

5. Conclusions

A single crystal of composition $[(Na_{0.5}K_{0.5})_{0.97}Li_{0.03}](Nb_{0.8}Ta_{0.2})O_3$ has been grown by the solid state crystal growth method. A crystal of between 20 and 50 μm thickness was grown on a ⟨0 0 1⟩-oriented $KTaO_3$ seed crystal. The crystal contained porosity incorporated from the matrix as the crystal grew. EDS analysis showed the single crystal to have the same composition as the matrix. A single crystal of constant thickness can be grown by adding a liquid phase sintering aid. The solid state crystal growth method is promising for the growth of single crystals of (Na, K, Li)(Nb, Ta)O_3.

Acknowledgements

This project was supported by the European Union under the Sixth Framework project IMMEDIATE and by the National project Electronic Ceramics, Nano, 2D in 3D Structures. The authors would like to thank J. Cilenšek, S. Drnovšek, A. Gross and V. Wesemann for technical support and T. Kenda for assistance with powder preparation.

References

1. Haertling, G. H., Ferroelectric ceramics: history and technology. *J. Am. Ceram. Soc.*, 1999, **82**(4), 797–818.
2. Kosec, M. and Kolar, D., On activated sintering and electrical properties of $NaKNbO_3$. *Mater. Res. Bull.*, 1975, **10**, 335–340.
3. Malic, B., Bernard, J., Holc, J., Jenko, D. and Kosec, M., Alkaline-earth doping in (K, Na)NbO_3 based piezoceramics. *J. Eur. Ceram. Soc.*, 2005, **25**, 2707–2711.
4. Saito, Y., Takao, H., Tani, T., Nonoyama, T., Takatori, K., Homma, T. *et al.*, Lead-free piezoceramics. *Nature*, 2004, **432**, 84–87.
5. Wada, S., Muraoka, K., Kakemoto, H., Tsurumi, T. and Kumagai, H., Enhanced piezoelectric properties of potassium niobate single crystals by domain engineering. *Jpn. J. Appl. Phys.*, 2004, **43**(9B), 6692–6700.
6. Ahtee, M. and Glazer, A. M., Lattice parameters and tilted octahedra in sodium-potassium niobate solid solution. *Acta Cryst.*, 1976, **A32**, 434–446.
7. Fisher, J. G., Benčan, A., Holc, J., Kosec, M., Vernay, A. S. and Rytz, D., Growth of $(Na_{0.5}K_{0.5})NbO_3$ single crystals by solid state crystal growth. *J. Cryst. Growth*, 2007, **303**, 487–492.
8. Matsubara, M., Yamaguchi, T., Sakamoto, W., Kikuta, K., Yogo, T. and Hirano, S. I., Processing and piezoelectric properties of lead-free (K, Na) (Nb, Ta)O_3 ceramics. *J. Am. Ceram. Soc.*, 2005, **88**(5), 1190–1196.
9. Samardžija, Z., Bernik, S., Marinenko, R. B., Malič, B. and Čeh, M., An EPMA study on $KNbO_3$ and $NaNbO_3$ single crystals—potential reference materials for quantitative microanalysis. *Mikrochim. Acta*, 2004, **145**, 203–208.
10. Chiang, Y. M., Birnie, D. and Kingery, W. D., *Physical Ceramics: Principles for Ceramic Science and Engineering*. John Wiley and Sons, New York, 1997, p. 374.
11. Jung, Y. I., Choi, S. Y. and Kang, S.-J. L., Grain-growth behavior during stepwise sintering of barium titanate in hydrogen gas and air. *J. Am. Ceram. Soc.*, 2003, **86**(12), 2228–2230.
12. Oh, K. S., Jun, J. Y., Kim, D. Y. and Hwang, N. M., Shape dependance of the coarsening behavior of niobium carbide grains dispersed in a liquid iron matrix. *J. Am. Ceram. Soc.*, 2000, **83**(12), 3117–3120.
13. Chung, S. Y., Yoon, D. Y. and Kang, S.-J. L., Effects of donor concentration and oxygen partial pressure on interface morphology and grain growth behavior in $SrTiO_3$. *Acta Mater.*, 2002, **50**, 3361–3371.
14. van der Eerden, J. P., Crystal growth mechanisms. In *Handbook of Crystal Growth. 1 Fundamentals Part A: Thermodynamics and Kinetics*, ed. D. T. J. Hurle. North-Holland, Amsterdam, 1993, pp. 311–475.
15. Jenko, D., Benčan, A., Malič, B., Holc, J. and Kosec, M., Electron microscopy studies of potassium sodium niobate ceramics. *Microsc. Microanal.*, 2005, **11**, 572–580.